Monatshefte für Chemie - Chemical Monthly
https://doi.org/10.1007/s00706-020-02702-6

ORIGINAL PAPER

New tripodal ligand on the triphenylphosphine oxide platform with 1,2,3-triazole side arms: synthesis, structure, coordination, and extraction properties

Igor Y. Kudryavtsev[1] · Olga V. Bykhovskaya[1] · Anna G. Matveeva[1] · Tatyana V. Baulina[1] · Margarita P. Pasechnik[1] · Sergey V. Matveev[1] · Anna V. Vologzhanina[1] · Alexander N. Turanov[2] · Vasilii K. Karandashev[3,4] · Valery K. Brel[1]

Received: 31 July 2020 / Accepted: 30 September 2020

Abstract

New hybrid tripodal propeller ligands on the triphenylphosphine oxide platform with triazole rings in the side arms and alkyl and aryl substituents in the triazole fragments have been synthesized by the click reaction. Composition and structure of the prepared compounds have been established by vibrational (IR, Raman) and multinuclear (^{1}H, ^{13}C, ^{31}P) NMR spectroscopy, elemental analysis, and mass spectrometry. Coordination and extraction properties of the prepared compounds toward Pd(II) have been studied by the example of one of the ligands.

Graphic abstract

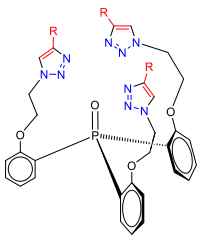

Keywords Click reaction · Extraction · 1,2,3-Triazole · Tripodal ligands · Palladium complex · X-ray structure determination

Introduction

Versatile architecture of tripodal ligands based on central core (platform) and three side arms containing functional groups provides a possibility to construct various hosts of different denticity and geometry [1, 2]. Depending on the nature of functional groups, tripodal ligands can form complexes with cations [3–6], anions [7–10], and neutral molecules [11–13]. These ligands are used for recovery of *d*- and *f*-block elements and separation of actinides and lanthanides [10, 14–18]. At the same time, there is growing interest in tripodal ligands based on the triphenylphosphine oxide platform [19–22]. Due to structural features, these ligands adopt a propeller conformation, where the side chains in the *ortho* position with donor groups come close to each other

Electronic supplementary material The online version of this article (https://doi.org/10.1007/s00706-020-02702-6) contains supplementary material, which is available to authorized users.

✉ Igor Y. Kudryavtsev
zaq@ineos.ac.ru

[1] Nesmeyanov Institute of Organoelement Compounds, Russian Academy of Sciences, Moscow, Russia

[2] Institute of Solid State Physics, Russian Academy of Sciences, Chernogolovka, Russia

[3] Institute of Microelectronics Technology Problems and High Purity Materials, Russian Academy of Sciences, Chernogolovka, Russia

[4] National University of Science and Technology MISiS, Moscow, Russia

Published online: 17 October 2020

and the central P=O group to form a cavity favorable for complexation with metal cation. These ligands containing C=O and C≡N groups in the side chains produce complexes with *d*- and *f*-block elements [19–22] and behave as efficient extractants for actinides and lanthanides [21, 22]. Designing polydentate ligands containing donor atoms of different nature and showing diverse affinity to different types of cations is the promising direction of tripodal ligands development. For example, the combination of N and O centers may provide ligand selectivity [23]. It is known that ligands containing 1,2,3-triazole fragments produce complexes with metal ions [24–26]. In this context, 1,2,3-triazole fragments are promising candidates to include in the side chains of tripodal ligands based on the triphenylphosphine oxide platform. Approaches to the synthesis of 1,2,3-triazoles are well developed [26–29]. Ligands containing 1,2,3-triazole fragments are known to form stable complexes with $PdCl_2$ [24, 30–33], compounds with these fragments recover palladium from aqueous solutions [34–36].

The aim of this work is to synthesize new tripodal N,O-donor ligands **1**–**6** based on the triphenylphosphine oxide platform with 1,2,3-triazole fragments in the side chains (Fig. 1) and to study their coordination and extraction properties toward palladium(II) by the example of compound **1**.

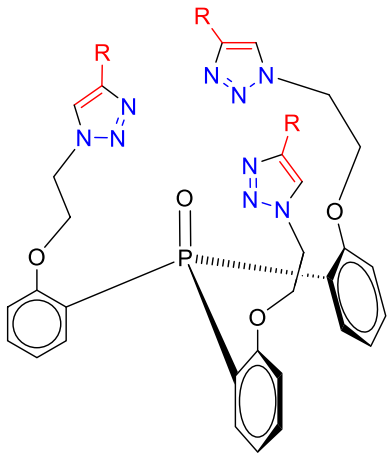

Fig. 1 Tripodal ligands **1**–**6**. R: **1**, Ph; **2**, 4-MeC_6H_4; **3**, 4-$MeOC_6H_4$; **4**, 4-*t*-BuC_6H_4; **5**, *n*-Bu; **6**, *n*-C_6H_{13}

Results and discussion

The target phosphine oxides **1**–**6** were prepared by the following general scheme (Scheme 1). Initial triphenyl phosphate was treated with lithium diisopropylamide (LDA) to give tris(2-hydroxyphenyl)phosphine oxide as a core compound. The reaction of the latter with 2-chloroethanol under alkaline conditions led to the corresponding hydroxyethyl derivative, which was converted via two stages into triazide **7** (the preparation of compound **7** was reported previously [37]). The click reaction of triazide **7** with the appropriate acetylenes in the presence of CuBr catalyst resulted in the target ligands **1**–**6** in good yields. The structure of the obtained compounds **1**–**6** was confirmed by ^{1}H, ^{13}C, ^{31}P NMR and IR spectroscopy, while the structure of compound **1** was established by X-ray crystallography.

Scheme 1

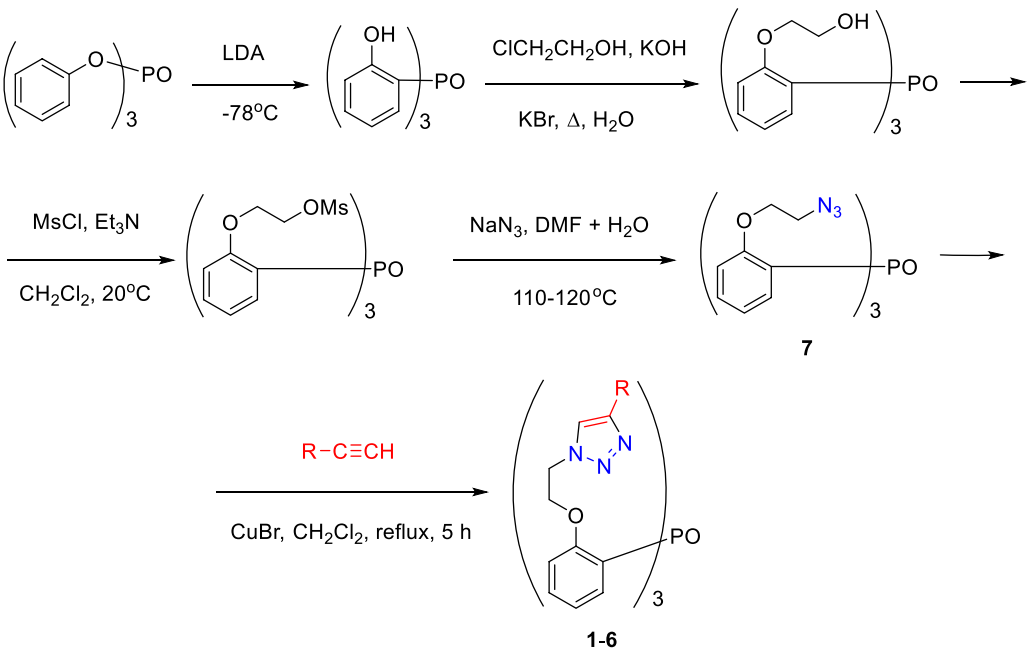

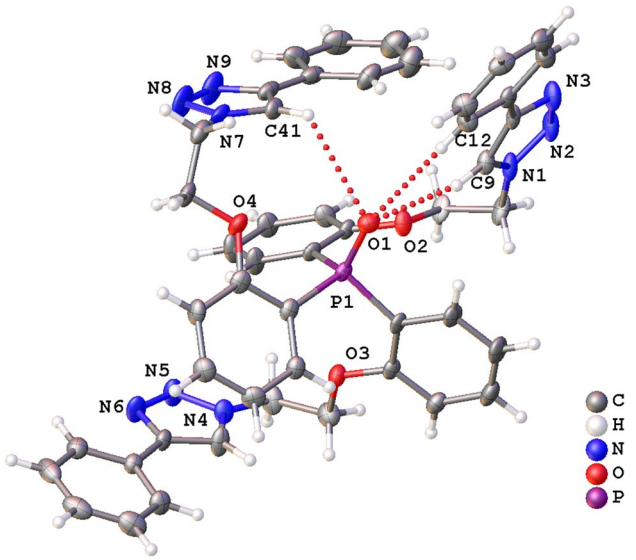

Fig. 2 Molecular view of compound **1** in representation of atoms with thermal ellipsoids ($p = 50\%$). Intramolecular hydrogen bonds are depicted with dashed line

The molecule structure in crystals of ligand **1** has asymmetrical propeller conformations (Fig. 2). Two of the three *ortho* OCH_2 substituents are oriented to the same direction as the P=O group, while the third substituent is oriented to the opposite direction. Bond distances and angles of ligand **1** (Table S1, ESI) are typical for related tripodal ligands with different functional groups in the side arms reported earlier [21, 38–41]. All these compounds have the 2-UP conformation. In this conformation, two of three *ortho* substituents are oriented to the same direction as the P = O group, while the third substituent is directed to the opposite side. For compound **1**, the O1–P1–C18–O3 angle of -171.83(2)° corresponds to the "arm" situated on the opposite side toward the vector of P=O bond, and two other "arms" are located on the same side as P=O phosphine oxide in respect to the carbon atoms of POC3 moiety with O–P–C–O angles equal to ca. 55°. In the tripodal ligands with hydroxyl [41] and tetrazole groups in the side arms [39], such conformation is additionally supported by two intramolecular O–H…O=P or N–H…O=P interactions, respectively. While three intramolecular C–H…O=P bonding in ligand **1** can be found with hydrogen atoms of two "arms" situated on the same side as the P=O group (Fig. 2). The C12–H…O1 bond between the phosphoryl group and the phenyl ring is as short as 3.68(1) Å (for the C…O distance); the C–H…O angle is 175.6(1)°. The C9–H…O1 distance is characterized by r(C…O) = 3.39(1) Å and C–H…O angle of 166.2(2)°. The C41–H…O1 distance is characterized by r(C…O)=3.68(1) Å and C–H…O angle of 130.4(2)°. Moreover, one can propose intramolecular π-stacking interaction between a benzene and a triazole rings of these arms (Fig. S1, ESI). The angle between meanplanes of the N7–N8–N9–C41–C42 and the C1–C2–C3–C4–C5–C6 rings is equal to 11.7(1)°, and intercentroid distance is equal to 3.99(2) Å. Intermolecular bonding includes C–H…N and C–H…π interactions; and the molecules packed so that solvent molecules (removed using SQUEEZE procedure) form infinite channels parallel with the crystallographic axis *c* (Fig. S2, ESI).

Let us note that the P=O bond (1.500(6) Å) is longer than that in the related 2-substituted triarylphosphine oxides containing no hydrogen bonds (for example, 1.485 Å in $[2\text{-}Bu_2NC(O)CH_2OC_6H_4]_3P(O)$ and 1.486 Å in $[2\text{-}Me_2NC(O)CH_2OC_6H_4]_3P(O)$ [21], but almost the same as in ligands, where P = O group is involved in hydrogen bonding: 1.502 Å for $Ph_2P(O)CH_2CH_2CH(OH)Me$ [42], 1.503 Å for $[2\text{-}HO(CH_2)_2OC_6H_4]_3PO$ [41], 1.513 Å for $(HOCH_2CH_2CH_2)_3PO$ [43]. The IR spectrum of crystalline phosphine oxide **1** shows absorption of the phosphoryl group ν(P=O) as a shoulder at about ~ 1175 cm^{-1}, which is slightly lower than for related compounds producing no intramolecular H-bond [21]; the band ν(C–H) is broad with a weak maximum at ~ 3130 cm^{-1}, which agrees well with the formation of intramolecular hydrogen bonds C–H•••O=P as revealed by X-ray diffraction. In the IR spectrum of solid compound **1**, a weak band at 1563 cm^{-1} (ν(C=C)) and medium-intensity band at 1037 cm^{-1} (ring deformation) can be related to triazole ring vibrations. The Raman spectrum proved to be more informative for the characterization of triazole rings: observed lines at 1555, 1358, and 1229 cm^{-1} may be referred to vibrations of the triazole rings by comparison with spectra of related compounds [44].

The IR spectra of the other obtained compounds are similar to that of ligand **1** (Table 1) which confirm their structures. Thus, the spectra of all compounds show ν(PO) bands at about ~ 1176 cm^{-1}, ν(C–H) bands at 3120–3133 cm^{-1} are broadened or split. One can suppose that in solid state in all obtained compounds, like in **1**, C–H protons produce contacts with either phosphoryl oxygen or other proton acceptors. Vibrations of double bonds of the triazole ring are characterized by the bands of different intensity at 1551–1560 cm^{-1}.

Table 1 Analytically important IR absorption bands of solid compounds **1**–**6** ($\bar{\nu}/cm^{-1}$; KBr disk)

Compound	ν(P=O)	ν(C–H)	Vibration of triazole moiety/ cm^{-1}
1	~1175m, sh	~3130w, sh	1560vw
2	1176m	3130w, 3128w	1560vw
3	1175m	3132w	1560 m
4	1179m	3132w, sh	1560w
5	1176m	3120w	1551w, 1530w
6	1176m	3123w	1551w

The structure of the obtained compounds **1**-**6** was confirmed also by ^{1}H, ^{13}C, and ^{31}P NMR spectroscopic data. The ^{1}H and ^{13}C NMR spectra of these compounds show signals typical for a triazole fragment. The ^{1}H NMR spectra of compounds **1**–**6** show singlet signals with δ_H at 8 ppm for compounds **1**–**4** (R=Ar) and at 7 ppm for compounds **5**, **6** (R=Alk) corresponding to the C–H proton of the triazole ring. Other proton signals are in the expected regions. The ^{13}C NMR spectra of compounds **1**–**6** display singlet signals at δ_C in the regions 122–123 ppm (CH) and 147–148 ppm (–C=) indicating the presence of –C=CH– fragment of the triazole ring. Other carbon resonances correspond to values typical for related compounds [37, 41].

By the example of compound **1**, we studied the extraction of Pd(II) from hydrochloric acid solutions into 1,2-dichloroethane (DCE) and the possibility of complex formation with $PdCl_2$.

Liquid–liquid extraction of Pd(II) with compound 1 from HCl solutions

To determine efficiency of Pd(II) recovery, we calculated the distribution ratios ($D_{Pd}=[Pd]_{org}/[Pd]_{aq}$) and extent of palladium recovery ($E\%=[Pd]_{org}/[Pd]_{init}\cdot 100\%$). The dependence of $E\%$ on the concentration of HCl in the aqueous phase is shown in Fig. 3. Recovery extent from aqueous solutions reaches 90–99% palladium at acid concentrations below 0.5 M. However, recovery efficiency sharply decreases at HCl concentration higher than 2 M. This is due to the high stability of $[PdCl_4]^{2-}$ complexes in the aqueous phase. The effect of HCl concentration in aqueous phase on the extraction of Pd(II) with solutions of compound **1** in DCE is shown in Fig. 4.

The extraction efficiency was found to decrease as [HCl] increases. Furthermore, the dependence of D_{Pd} upon $[H^+]$ at a fixed concentration of Cl^- ions was studied. As shown in Fig. 5, variation of $[H^+]$ did not affect the Pd(II) extraction with compound **1**. On the other hand, an increase in $[Cl^-]$ at a fixed concentration of H^+ leads to decrease of the D_{Pd} values (Fig. 6).

In the extraction systems with compound **1**, the plot of $\log D_{Pd}$ vs. $\log[Cl^-]$ exhibited a straight line with a slope close to −2, which means that two Cl^- ions were released in

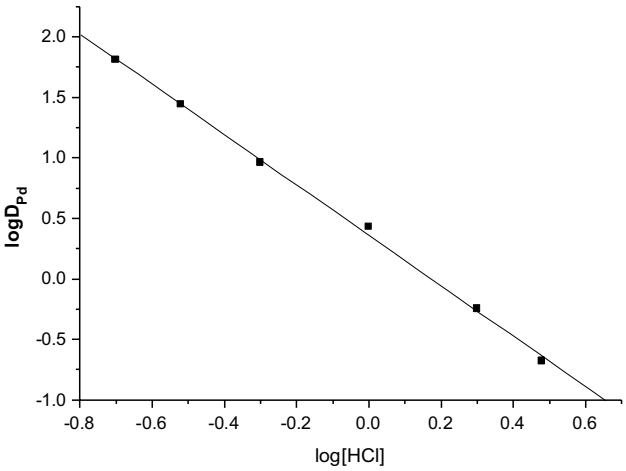

Fig. 4 Effect of HCl concentration in aqueous phase on the extraction of Pd(II) with 0.001 M solution of compound **1** in DCE. Exp. data black square, solid line: linear regression ($R=0.999$). Calculated slope value is -2.08 ± 0.04

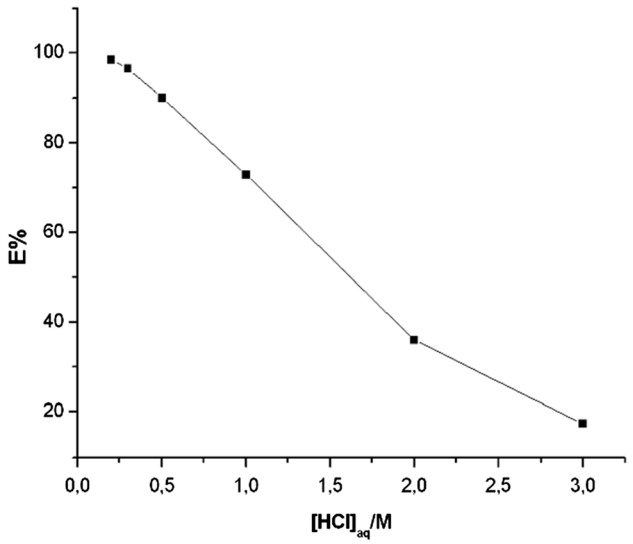

Fig. 3 Dependence of $E\%$ on the concentration of HCl in the aqueous phase for Pd(II) extraction with 0.001 M solution of compound **1**. Exp. data black square

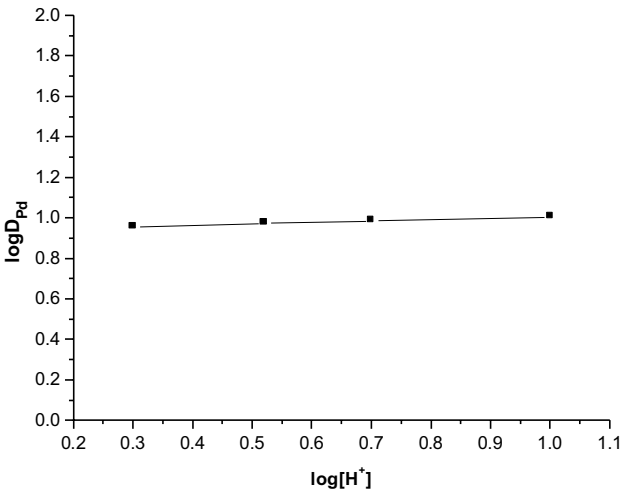

Fig. 5 Effect of $[H^+]$ concentration in aqueous phase on the extraction of Pd(II) with 0.001 M solutions of compound **1** in DCE. Concentration of $[Cl^-]$ is 0.5 M. Exp. data black square, solid line: linear regression ($R=0.996$)

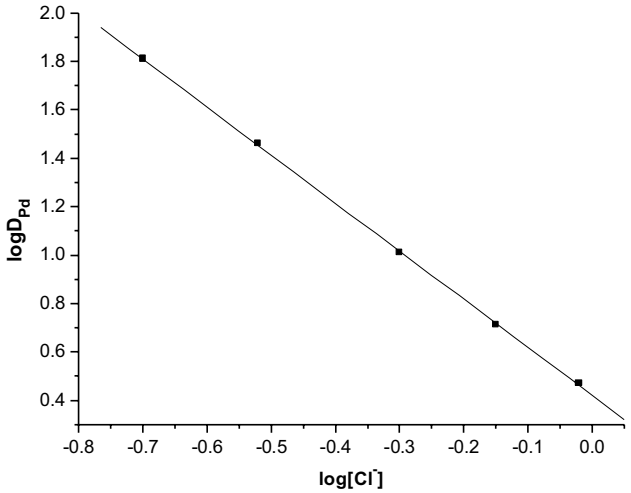

Fig. 6 Effect of [Cl^-] concentration in aqueous phase on the extraction of Pd(II) with 0.001 M solutions of compound **1** in DCE. Concentration of [H^+] is 0.1 M. Exp. data black square, solid line: linear regression ($R = 0.999$). Calculated slope value is -1.98 ± 0.02

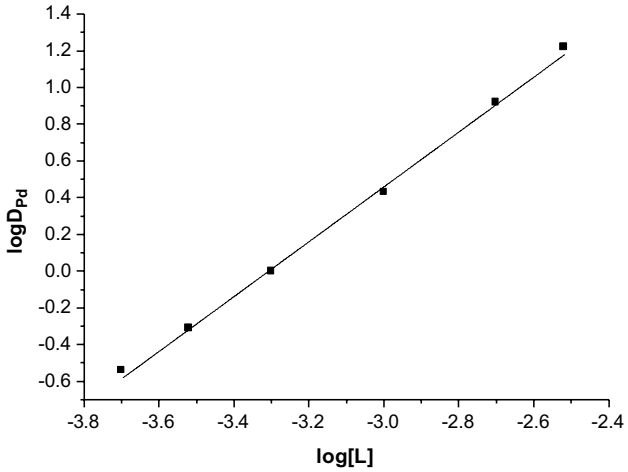

Fig. 7 Effect of extractant **1** concentration in DCE on the extraction of Pd(II), from 1.0 M HCl solution. Exp. data black square, solid line: linear regression ($R = 0.999$). Calculated slope value is 1.49 ± 0.03

the extraction reaction. When [HCl] > 0.1 M, Pd(II) preferably exists in aqueous solutions as $[PdCl_4]^{2-}$ anion. Therefore, Pd(II) is extracted into organic phase as $[PdCl_2L_s]^0$ complex (where *s* is a Pd:L stoichiometric ratio) via the substitution of two Cl^- ions in $[PdCl_4]^{2-}$ anion by *s* coordinated molecules of ligand L.

The stoichiometric ratio of palladium(II) to extractant in the extracted complexes was determined by the slope analysis method. The variations in D_{Pd} as a function of compound **1** concentration in DCE are shown in Fig. 7. At constant composition of the aqueous phase, the slope of dependence $\log D_{Pd}$ vs. log[L] is close to 1.5, which corresponds to Pd(II) transfer into organic phase as neutral complexes of composition $[PdLCl_2]^0$ and $[PdL_2Cl_2]^0$.

Taking into account the found stoichiometric ratios, Pd(II) extraction from HCl solutions with compound **1** into DCE can be described by Eqs. (1, 2):

$$\left[PdCl_4\right]^{2-}_{(aq)} + L_{(org)} \rightleftarrows \left[PdLCl_2\right]^{0}_{(org)} + 2Cl^-_{(-aq)}, K_1 \qquad (1)$$

$$\left[PdCl_4\right]^{2-}_{(aq)} + 2L_{(org)} \rightleftarrows \left[PdL_2Cl_2\right]^{0}_{(org)} + 2Cl^-_{(aq)}, K_2, \qquad (2)$$

where symbols (org) and (aq) designate the components of organic and aqueous phases, respectively, K_1 and K_2 are equilibrium constants of palladium extraction. The values of equilibrium constants K_1 and K_2, calculated from the data of Fig. 7 are equal to $(1.22 \pm 0.03) \times 10^3$ and $(1.45 \pm 0.03) \times 10^6$, respectively.

Thus, tripodal ligand **1** efficiently extracts Pd(II) from hydrochloric acid solutions into DCE. The extracted complexes have the composition $[Pd(L)Cl_2]$ and $[Pd(L)_2Cl_2]$. According to available literature data on the structure of complexes of substituted 1,2,3-triazoles with $PdCl_2$ [24, 30–33], one can suppose that ligand **1** is coordinated in the complex with composition Pd:L = 1:1 in an *N*,*N*-bidentate mode, while both ligand molecules in the 1 : 2 complex are coordinated in *N*-monodentate mode. To verify this assumption, we prepared the complex of composition Pd:L = 1:1.

Complexation of ligand 1 with $PdCl_2$

The reaction of stoichiometric amounts of $PdCl_2(NCPh)_2$ with **1** in acetonitrile resulted in the formation of a precipitate. The composition of the resultant compound **8** according to elemental analysis and vibrational spectroscopy (vide infra) corresponds to $[PdCl_2(\mathbf{1})]\cdot 3H_2O$ (Scheme 2). The complex is insoluble in common solvents used for NMR spectroscopy ($CDCl_3$, CD_3CN). The complex undergoes solvolysis in DMSO-d_6 solution according to NMR spectroscopic data (^1H, ^{31}P, ^{13}C).

The data of the vibrational spectra for the solid complex and ligand are presented in Table 2. In the IR spectrum of the complex, ν(P=O) band retains its position as compared with the band of the free ligand, which indicates that the phosphoryl group is not involved in coordination. The band ν(C–H) slightly changes its shape and its maximum is shifted to 3137 cm^{-1}. Furthermore, the intensity of absorption band at 1037 cm^{-1} related to ring deformation decreases and an absorption at 1065 cm^{-1} appeared. In the Raman spectrum,

Scheme 2

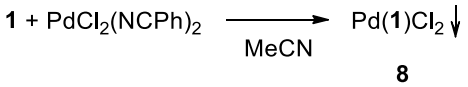

Table 2 Main vibration frequencies for ligand **1** and its complex **8** ($\bar{\nu}$/cm^{-1})

Compound	ν(P=O)	ν(C–H)	ν(triazole)		ν(Pd–N)	ν(Pd–Cl)	
	IR	IR	IR	Raman	IR	IR	Raman
1	1175sh	3130w	1037m	1555, 1358, 1229			
8	1175sh	3137w	1065sh	1558, 1373, 1236	~ 495br	345br	301, 342

the lines related to vibrations of the triazole ring are shifted in different extent to the high-frequency region, which indicates the participation of the nitrogen atom of the triazole ring in coordination with Pd(II) cation. The vibrations of coordinated to Pd(II) chloride ions appear in the vibrational spectra of complex **8** as a split band at 301 and 342 cm^{-1} in the Raman spectrum and at ~ 345 cm^{-1} in the IR spectrum, which is typical for *cis* complexes of $PdCl_2$ [44, 45]. The band at 495 cm^{-1} observed in IR spectrum can be related to a ν(Pd–N) vibration [44]. It is known that the palladium(II) complexes have a square planar geometry, typical for complexes with d^8 configuration, the coordination number of Pd(II) is four [24, 30–33, 44]. The body of experimental data allows us to assume that compound **8** is a neutral *cis* complex of $PdCl_2$ with ligand **1** molecule coordinated in *N*,*N*-bidentate mode.

Conclusion

Six new tripodal ligands based on the triphenylphosphine oxide platform with 1,2,3-triazole fragments in side arms and different alkyl and aryl substituents attached to the triazole rings were synthesized by click reaction in good yields. The coordination and extraction properties of the new type of tripodal ligands were studied by the example of ligand **1**. Compound **1** was found to recover efficiently (up to 99%) Pd(II) from hydrochloric acid solutions into 1,2-dichloroethane. The extracted complexes were revealed to have a composition [Pd(**1**)Cl_2] and [Pd(**1**)$_2Cl_2$]. The model 1:1 complex of ligand **1** with $PdCl_2$ was isolated. The body of experimental data (IR and Raman spectroscopy, elemental analysis) allows us to assume that compound **8** is a neutral *cis* complex of $PdCl_2$ with ligand **1** coordinated in *N*,*N*-bidentate mode.

Experimental

Organic solvents used in the work were purified by standard procedures [46]. $CDCl_3$ (99.8% D, Sigma-Aldrich) was used as received. ^{1}H, ^{13}C{^{1}H}, and ^{31}P{^{1}H} NMR spectra in $CDCl_3$ were recorded on a Bruker Avance 400 spectrometer operating at 400.13, 100.61, and 161.98 MHz, respectively. Chemical shifts (ppm) refer to the residual protic solvent peaks (for ^{1}H and ^{13}C) and 85% H_3PO_4 (for ^{31}P{^{1}H}) as external standards and coupling constants are expressed in Hertz (Hz). IR spectra in the region 400-4000 cm^{-1} were obtained on a Bruker Tensor 37 FTIR spectrometer. The solid samples were KBr pellets and mulls in Nujol. Raman spectra in the range of 100-3500 cm^{-1} were recorded on a Jobin–Yvon LabRAM 300 spectrometer, equipped with a microscope and laser CCD detector. The He–Ne laser emission line at 632.8 nm was used for excitation at a power not higher than 2 mW. Mass spectra for solutions of compounds in methanol were recorded on an AmaZon Bruker Daltonik GmbH mass spectrometer in Ultra-Scan mode with positive ionization, detected range was *m/z* = 70–2200. The content of C, H, and N was determined on a Carlo Erba 1106 instrument. The content of P was determined according to the published procedures [47]. Melting points were determined in open capillary tubes on a Stanford Research Systems MPA120 EZ-melt automated melting point apparatus.

Tris[2-(2′-azidoethoxyphenyl)phosphine oxide (**7**) was prepared by a literature procedure [37]. Acetylenes RC≡CH (R=Ph, 4-MeC_6H_4, 4-MeOC_6H_4, 4-*t*-BuC_6H_4, *n*-Bu, *n*-C_6H_{13}) were purchased from Aldrich and were used as received. Salts $PdCl_2$ (pure grade), NaCl (pure grade), $PdCl_2(NCPh)_2$ (Aldrich) were used without further purification. The following reagents were used for the preparation of solutions in the extraction study: bidistilled water, 1,2-dichloroethane (reagent grade), HCl (high purity grade). Solutions for spectral and extraction studies were prepared by volumetric/gravimetric method.

X-ray crystallography

Intensities of the reflections for compound **1** were collected on a Bruker Apex DUO CCD diffractometer using CuKα radiation (λ = 1.54178 Å; monochromatted with multilayered optics) at 120.0(2) K. The structure was solved by ShelXT method [48] and refined by full-matrix least squares against F^2. Non-hydrogen atoms were refined anisotropically. Positions of hydrogen atoms were calculated and all hydrogen atoms were included in the refinement by a riding model with U_{iso}(H) = 1.2 U_{eq}(X). Single crystal contains highly disordered solvent molecules which have been treated as a diffuse contribution to the overall scattering without the specific atom positions by SQUEEZE/PLATON [49]. All calculations were made using the SHELXL2014 [50] and OLEX2 [51] program packages. Crystal parameters and refinement details are listed in Table 3. CCDC 2018462 contains the supplementary crystallographic data for compound **1**. These

Table 3 Crystal parameters and refinement details for compound **1**

	1 [solvent]
Formula	$C_{48}H_{42}N_9O_4P$
Formula weight	839.87
Space group	*P* 2$_1$/*n*
a/Å	11.84(5)
b/Å	31.95(8)
c/Å	12.20(4)
β/°	98.9(3)
V (Å^3)	4560(27)
Z	4
μ/mm^{-1}	0.965
d_{calc}/g cm^{-3}	1.223
F(000)	1760
No. of measured refls.	29,128
No. of independent refls. (R_{int})	7961 (0.104)
No. of observed rfls. [$I > 2\sigma(I)$]	6091
No. of parameters	559
Goodness-of-fit	1.07
R_1 [$I > 2\sigma(I)$]	0.085
wR_2 [all data]	0.213
$\Delta\rho_{max}$, $\Delta\rho_{min}$/e Å^{-3}	0.81, −0.70

data can be obtained free of charge via http://www.ccdc.cam.ac.uk/structures/, or from the Cambridge Crystallographic Data Centre, 12 Union Road, Cambridge CB2 1EZ, UK; fax: (+44) 1223-336-033; or e-mail: deposit@ccdc.cam.ac.uk.

General procedure for synthesis of tris[2-[2′-(4″-R-1″,2″,3″-triazol-1″-yl)ethoxy]phenyl]phosphine oxides 1-6

A mixture of 0.28 mmol of tris[2-(2′-azidoethoxy)phenyl] phosphine oxide **7**, 1.68 mmol of the corresponding substituted acetylene, 0.028 mmol of CuBr, and 3 cm^3 of CH_2Cl_2, was heated under reflux for 5 h. The product was isolated by chromatography on SiO_2 or Al_2O_3 using chloroform–methanol (20:1) mixture as an eluent. The eluate was evaporated to dryness and the solid residue was triturated with warm ether to give tris[2-[2′-(4″-R-1″,2″,3″-triazol-1″-yl)ethoxy]phenyl] phosphine oxides **1**–**6** in 70–91% yield as powders. Numbering scheme for compounds **1**–**6** is given in Scheme 3.

Tris[2-[2′-(4″-phenyl-1″,2″,3″-triazol-1″-yl)ethoxy]phenyl]-phosphine oxide (1, $C_{48}H_{42}N_9O_4P$) White powder; yield 70%; *T*. decomp.: > 115 °C; IR (KBr disk): $\bar{\nu}$ = 3338br, 3130w,sh, 3080sh, 3066m, 3029sh, 2997sh, 2951sh, 2880vw, 2851vw, 1589s, 1575m, 1563vw, 1477m, 1441vs, 1390vw, 1368vw, 1284s, 1232s, 1175m,sh, 1165m, 1139m, 1085m, 1049sh, 1037m, 970w, 909vw, 849vw, 801w, 761vs, 696s, 610vw, 557m, 520w cm^{-1}; Raman: $\bar{\nu}$ = ~ 3140vw, 3064m, 2952vw, 2880vw, 1610vs, 1555m, 1470vw, 1442vw, 1358m, 1229w, 1176w, 1074vw, 1042m, 1000s, 971s, 910vw, 799vw, 770vw, 667m, 610vw cm^{-1}; ^{1}H NMR (400.13 MHz, $CDCl_3$): δ = 4.12 and 4.24 (12H, both s, H$^{1'}$, H$^{2'}$), 6.67 (3H, dd, $^3J_{HH}$ = 8.4 Hz, $^4J_{HH}$ = 5.2 Hz, H^3), 6.88 (3H, t, $^3J_{HH}$ = 7.6 Hz, H^5), 7.20–7.45 (15H, m, H^4, H^6, H$^{3'''}$, H$^{4'''}$, H$^{5'''}$), 7.67 (6H, d, $^3J_{HH}$ = 6.0 Hz, H$^{2'''}$, H$^{6'''}$), 8.12 (3H, s, H$^{5''}$) ppm; ^{13}C NMR (100.61 MHz, $CDCl_3$): δ = 49.12 (C$^{2'}$), 66.74 (C$^{1'}$), 111.93 (d, $^3J_{PC}$ = 6.0 Hz, C^3), 120.74 (d, $^1J_{PC}$ = 109.7 Hz, C^1), 121.61 (d, $^3J_{PC}$ = 13.1 Hz, C^5), 122. 08 (C$^{5''}$), 125.73 (C$^{2'''}$, C$^{6'''}$), 127.92 (C$^{4'''}$), 128.63 (C$^{3'''}$, C$^{5'''}$), 130.65 (C$^{1'''}$), 133.91 (d, $^2J_{PC}$ = 8.0 Hz, C^6), 134.04 (C^4), 147.51 (C$^{4''}$), 159.59 (C^2) ppm; ^{31}P{^{1}H} NMR (161.98 MHz, $CDCl_3$): δ = 25.6 ppm; MS: *m*/*z* = 840 ([M]$^+$).

Tris[2-[2′-(4″-(4‴-methylphenyl)-1″,2″,3″-triazol-1″-yl)-ethoxy]phenyl]phosphine oxide (2,$C_{51}H_{48}N_9O_4P$) White powder; yield 77%; *T*. decomp.: > 135 °C; IR (KBr disk): $\bar{\nu}$ = 3369br, 3130w, 3128w, 3077w, 2922w, 2879w, 1590s, 1576m, 1560vw, 1500m, 1479s, 1461m, 1441vs, 1389w, 1366w, 1284m, 1248m, 1230s, 1176m, 1162m, 1139m, 1086m, 1048m, 1033m, 972w, 905w, 824m, 798m, 759s, 704w, 667m, 521m cm^{-1}; ^{1}H NMR (400.13 MHz, $CDCl_3$): δ = 2.34 (9H, s, CH_3), 4.12 and 4.23 (12H, both s, H$^{1'}$, H$^{2'}$), 6.69 (3H, br s, H^3), 6.88 (3H, t, $^3J_{HH}$ = 7.4 Hz, H^5), 7.10 (6H, d, $^3J_{HH}$ = 7.6 Hz, H$^{2'''}$, H$^{6'''}$), 7.27–7.44 (6H, m, H^4, H^6), 7.55 (6H, d, $^3J_{HH}$ = 7.6 Hz, H$^{3'''}$, H$^{5'''}$), 8.03 (3H, s, H$^{5''}$) ppm; ^{13}C NMR (100.61 MHz, $CDCl_3$): δ = 21.30 (CH_3), 49.16 (C$^{2'}$), 66.90 (C$^{1'}$), 112.08 (d, $^3J_{PC}$ = 4.3 Hz, C^3), 120.79 (d, $^1J_{PC}$ = 159 Hz, C^1), 121.56, 121.69 (C^5, C$^{5''}$), 125.66 (C$^{2'''}$, C$^{6'''}$), 127.82 (C$^{4'''}$), 129.30 (C$^{3'''}$, C$^{5'''}$), 133.92, 134.05 (C^4, C^6), 137.72 (C$^{1'''}$), 147.66 (C$^{4''}$), 159.65 (C^2) ppm; ^{31}P{^{1}H} NMR (161.98 MHz, $CDCl_3$): δ = 25.3 ppm; MS: *m*/*z* = 882 ([M]$^+$).

Tris[2-[2′-(4″-(4‴-methoxyphenyl)-1″,2″,3″-triazol-1″-yl)-ethoxy]phenyl]phosphine oxide (3, $C_{51}H_{48}N_9O_7P$) White powder; yield 70%; *T*. decomp.: > 130 °C; IR (KBr disk): $\bar{\nu}$ = 3393br, 3132w, 3080w, 3068w, 2997w, 2933w, 2835w, 1618m, 1590m, 1577m, 1560m, 1500s, 1478m, 1465m, 1441s, 1368w, 1303w, 1284m, 1248vs, 1175m, 1165sh, 1139m, 1108w, 1085m, 1030m, 972w, 909w, 837m, 797m, 757m, 697w, 662vw, 599w, 557m, 534m cm^{-1}; ^{1}H NMR (400.13 MHz, $CDCl_3$): δ = 3.80 (9H, s, CH_3), 4.09 and

Scheme 3

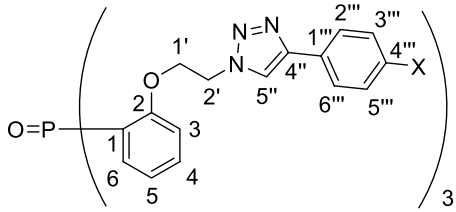

4.20 (12H, both s, $H^{1'}$, $H^{2'}$), 6.68 (3H, dd, $^3J_{HH}$ = 8.4 Hz, $^4J_{HH}$ = 4.8 Hz, H^3), 6.81 (6H, d, $^3J_{HH}$ = 8.4 Hz, $H^{3'''}$, $H^{5'''}$), 6.88 (3H, t, $^3J_{HH}$ = 7.4 Hz, H^5), 7.29–7.41 (6H, m, H^4, H^6), 7.58 (6H, d, $^3J_{HH}$ = 8.4 Hz, $H^{2'''}$, $H^{6'''}$), 8.01 (3H, s, $H^{5''}$) ppm; ^{13}C NMR (100.61 MHz, $CDCl_3$): δ = 49.17 ($C^{2'}$), 55.38 (CH_3), 66.82 ($C^{1'}$), 111.97 (d, $^3J_{PC}$ = 6.0 Hz, C^3), 114.04 ($C^{3'''}$, $C^{5'''}$), 120.65 (d, $^1J_{PC}$ = 109.7 Hz, C^1), 121.34 ($C^{5''}$), 121.66 (d, $^3J_{PC}$ = 12.1 Hz, C^5), 123.25 ($C^{1'''}$), 127.07 ($C^{2'''}$, $C^{6'''}$), 133.96 (d, $^2J_{PC}$ = 9.1 Hz, C^6), 134.08 (C^4), 147.36 ($C^{4''}$), 159.44 ($C^{4'''}$), 159.60 (C^2) ppm; ^{31}P{^{1}H} NMR (161.98 MHz, $CDCl_3$): δ = 25.2 ppm; MS: *m/z* = 930 ($[M]^+$).

Tris[2-[2′-(4″-(4‴-*tert*-butylphenyl)-1″,2″,3″-triazol-1″-yl)-ethoxy]phenyl]phosphine oxide (4, $C_{60}H_{66}N_9O_4P$) White powder; yield 91%; m.p.: 195–196 °C (CH_2Cl_2–ether); IR (KBr disk): $\bar{\nu}$ = 3400br, 3132w sh, 3090w, 3074w, 2961vs, 2920sh, 2868m, 1590s, 1575m, 1560w, 1496m, 1478s, 1462m, 1442vs, 1392w, 1366m, 1283s, 1240s, 1179m, 1165m, 1140m, 1112w, 1084m, 1050m, 1035m, 973w, 911vw, 841m, 799m 760vs, 702w, 557s, 522w cm^{-1}; ^{1}H NMR (400.13mHz, $CDCl_3$): δ = 1.31 (27H, s, CH_3), 4.08 and 4.19 (12H, both s, $H^{1'}$, $H^{2'}$), 6.64 (3H, dd, $^3J_{HH}$ = 7.8 Hz, $^4J_{HP}$ = 5.0 Hz, H^3), 6.87 (3H, t, $^3J_{HH}$ = 7.2 Hz, H^5), 7.30 (6H, d, $^3J_{HH}$ = 8.0 Hz, $H^{3'''}$, $H^{5'''}$, signal of H^4 is overlapped with the doublet of $H^{3'''}$ and $H^{5'''}$), 7.37 (3H, dd, $^3J_{HH}$ = 6.8 Hz, $^3J_{HP}$ = 14.4 Hz, H^6), 7.59 (6H, d,$^3J_{HH}$ = 8.0 Hz, $H^{2'''}$, $H^{6'''}$), 8.06 (3H, $H^{5''}$) ppm; ^{13}C NMR (100.61mHz, $CDCl_3$): δ = 31.34 (CH_3); 34.63 (C^{t-Bu}), 49.06 ($C^{2'}$), 66.71 ($C^{1'}$), 111.93 (d, $^3J_{PC}$ = 6.1 Hz, C^3), 121.64 (d, $^3J_{PC}$ = 12.3 Hz, C^5), 121.84 ($C^{5''}$), 125.53 ($C^{2'''}$, $C^{3'''}$, $C^{5'''}$, $C^{6'''}$), 127.84 ($C^{4'''}$), 133.9 (C^4), 134.0 (d, $^2J_{PC}$ = 1.8 Hz, C^6), 147.61 ($C^{4''}$), 150.99 ($C^{1'''}$), 159.61 (C^2) ppm; ^{31}P{^{1}H} NMR (161.98 MHz, $CDCl_3$): δ = 24.9 ppm; MS: *m/z* = 1009 ($[M]^+$).

Tris[2-[2′-(4″-butyl-1″,2″,3″-triazol-1″-yl)ethoxy]phenyl]-phosphine oxide (5, $C_{42}H_{54}N_9O_4P$) White powder; yield 70%; m.p.: 136-138 °C; IR (KBr disk): $\bar{\nu}$ = 3404br, 3120w, 3069m, 2957s, 2932s, 2872m, 2219w, 1686m, 1590vs, 1576s, 1551w, 1530w, 1479s, 1442vs, 1372m, 1284s, 1241s, 1176m, 1167m, 1141m, 1086m, 1045s, 911m, 847w, 799m, 759s, 732s, 705m, 644w, 608w, 557s, 521m cm^{-1}; ^{1}H NMR (400.13 MHz, $CDCl_3$): δ = 0.86 (9H, t, CH_3, $^3J_{HH}$ = 7.2 Hz), 1.28 (6H, sext, CH_2, $^3J_{HH}$ = 7.3 Hz, CH_2), 1.50 (6H, quin CH_2, $^3J_{HH}$ = 7.5 Hz), 2.49 (6H, t, CH_2, $^3J_{HH}$ = 7.8 Hz), 4.21 (12H, br s, $H^{1'}$, $H^{2'}$), 6.89 (3H, dd, $^3J_{HH}$ = 8.4 Hz, $^4J_{PH}$ = 5.2 Hz, H^3), 6.99 (3H, t, $^3J_{HH}$ = 7.6 Hz, H^5), 7.33 (3H, s, $H^{5''}$); 7.41–7.57 (6H, m, H^4, H^6) ppm; ^{13}C NMR (100.61 MHz, $CDCl_3$): δ = 13.81 (CH_3), 22.34, 25.29, 31.53 (CH_2), 48.98 ($C^{2'}$), 67.55 ($C^{1'}$), 112.56 (d, $^3J_{PC}$ = 7.0 Hz, C^3), 121.44 (d, $^1J_{PC}$ = 110.7 Hz, C^1), 121.70 (d, $^3J_{PC}$ = 13.1 Hz, C^5), 122.28 ($C^{5''}$), 133.96 (C^4), 134.30 (d, $^2J_{PC}$ = 8.0 Hz, C^6), 148.26 ($C^{4''}$), 159.99 (C^2) ppm; ^{31}P{^{1}H} NMR (161.98 MHz, $CDCl_3$): δ = 24.4 ppm; MS: *m/z* = 780 ($[M]^+$).

Tris[2-[2′-(4″-hexyl-1″,2″,3″-triazol-1″-yl)ethoxy]phenyl]-phosphine oxide (6, $C_{48}H_{66}N_9O_4P$) White powder; yield 75%; m.p.: 114–116 °C; IR (KBr disk): $\bar{\nu}$ = 3419br, 3123w, 3068m, 2928vs, 2857s, 1715vw, 1590vs, 1576s, 1551w, 1479s, 1442vs, 1395w, 1368m, 1284vs, 1241vs, 1176m, 1166m, 1140m, 1086m, 1045s, 910m, 846w, 799m, 758s, 705m, 666сл, 608w, 557s, 522m cm^{-1}; ^{1}H NMR (400.13 MHz, $CDCl_3$): δ = 0.85 (9H, t, $^3J_{HH}$ = 6.4 Hz, CH_3), 1.25 (18H, br s, CH_2), 1.52 (6H, br s, CH_2), 2.49 (6H, t, $^3J_{HH}$ = 7.4 Hz, CH_2), 4.22 (12H, br s, $H^{1'}$, $H^{2'}$), 6.90 (3H, br s, H^3), 7.00 (3H, t, $^3J_{HH}$ = 6.6 Hz, H^5), 7.33 (3H, s, $H^{5''}$), 7.41–7.58 (6H, m, H^4, H^6) ppm; ^{13}C NMR (100.61 MHz, $CDCl_3$): δ = 14.08 (CH_3), 22.57, 25.63, 29.01, 29.46, 31.57 (CH_2), 49.00 ($C^{2'}$), 67.54 ($C^{1'}$), 112.57 (d, $^3J_{PC}$ = 6.0 Hz, C^3), 121.40 (d, $^1J_{PC}$ = 109.7 Hz, C^1), 121.71 (d, $^3J_{PC}$ = 13.1 Hz, C^5), 122.28 ($C^{5''}$), 133.98 (C^4), 134.30 (d, $^2J_{PC}$ = 9.1 Hz, C^6), 148.27 ($C^{4''}$), 159.99 (C^2) ppm; ^{31}P{^{1}H} NMR (161.98 MHz, $CDCl_3$): 24.5 ppm; MS: *m/z* = 864 ($[M]^+$).

Synthesis of palladium complex of ligand 1 $[Pd(1)Cl_2]\cdot 3H_2O$ (8) A solution of 0.0180 g $[PdCl_2(NCPh)_2]$ (0.0476) mmol) in 1.5 cm^3 of acetonitrile was slowly added with stirring to a solution of 0.0400 g of ligand **1** (0.0476 mmol) in 3 cm^3 of acetonitrile. Upon addition of the salt, the reaction mixture immediately changed from a transparent solution to a cloudy mixture, which yielded a pale yellow precipitate. The precipitate was separated by decantation after 3 days. The powder was washed with acetonitrile and anhydrous ether and dried in vacuo (~ 1 Torr) at 62 °C to give 0.030 g (59%). *T*. decomp. > 240 °C; IR (KBr disk): $\bar{\nu}$ = 3350br, 3137w sh, 3065w, 2926w, 2101w, 1590s, 1577 m, 1560m, 1474s, 1442vs, 1375w, 1282s, 1235vs, 1175m, 1168m, 1140m, 1117sh, 1087m, ~ 1060sh, 1047m, 1005w, 912w, 799w, 763vs, 697s, 558m, 521w cm^{-1}; Raman: $\bar{\nu}$ = 3145vw, 3067w, 2960vw, 1612vs, 1593m, 1558m, 1443vw, 1373m, 1289vw,1236vw, 1164w, 1062w, 1045m, 1001s, 974m, 916vw, 849vw, 799vw, 768vw, 727vw, 670w, 620m, 407vw, 342m, 301s cm^{-1}.

Extraction of palladium(II)

1,2-Dichloroethane of reagent grade was used without additional purification as the organic solvent. The initial aqueous palladium(II) solutions were prepared by dissolving $PdCl_2$ in water, followed by the addition of HCl or NaCl. The initial concentrations of Pd(II) ions were 2×10^{-5} M. The phases were contacted at room temperature by agitation with a stirrer at 60 rpm for 1 h, which is sufficient to establish constant values of distribution ratios (D_{Pd}) at volume ratio of organic and aqueous phases of 1:1. The concentration of palladium(II) in the initial and equilibrated aqueous solutions was determined by mass spectrometry with the inductively coupled plasma ionization of samples (ICP-MS),

using a Thermo Scientific X-7 mass spectrometer. The content of Pd(II) in organic phase was determined as the difference in Pd(II) concentrations in aqueous phase before and after extraction. The distribution ratios for palladium were calculated as ratios of the equilibrium concentration in the organic and aqueous phases ($D_{Pd} = [Pd_{org}]/[Pd_{aq}]$). The error of the determined D_{Pd} values did not exceed 5%. The HCl concentration in equilibrium aqueous phase was determined by potentiometric titration with NaOH solution.

Acknowledgements The work was financially supported by the Russian Science Foundation (project no. 20–13–00329). Spectral studies were carried out using the equipment of the Center for Molecular Structure Studies, INEOS RAS.

References

1. Sahoo SK, Kim G-D, Choi H-J (2016) J Photochem Photobiol C Photochem Rev 30
2. Silva F, Fernandes C, Campello MPC, Paulo A (2017) Polyhedron 125:186
3. Lim J, Lynch VM, Edupuganti R, Ellington A, Anslyn EV (2016) Dalton Trans 45:10585
4. Phanopoulos A, Miller PW, Long NJ (2015) Coord Chem Rev 299:39
5. Batke S, Sietzen M, Wadepohl H, Ballmann J (2014) Inorg Chem 53:4144
6. Saad FA, Buurma NJ, Amoroso AJ, Knight JC, Kariuki BM (2012) Dalton Trans 41:4608
7. Gale PA (2011) Acc Chem Res 44:216
8. Khansari ME, Johnson CR, Basaran I, Nafis A, Wang J, Leszczynski J, Hossain MA (2015) RSC Adv 5:17606
9. Beletskiy EV, Wang XB, Kass SR (2016) J Phys Chem A 120:8309
10. Gale PA, Davis JT, Quesada R (2017) Chem Soc Rev 46:2497
11. Mazik M (2009) Chem Soc Rev 38:935
12. Stewart CD, Pedraza M, Arman H, Fan H-J, Schilling EL, Szpoganicz B, Musie GT (2015) J Inorg Biochem 149:25
13. Stewart CD, Arman H, Bawazir H, Musie GT (2014) Inorg Chem 53:10974
14. Leoncini A, Ansari SA, Mohapatra PK, Boda A, Ali SM, Sengupta A, Huskens J, Verboom W (2017) Dalton Trans 46:1431
15. Coburn KM, Hardy DA, Patterson MG, McGraw SN, Peruzzi MT, Boucher F, Beelen B, Sartain HT, Neils T, Lawrence CL, Staples RJ, Werner EJ, Biros SM (2016) Inorg Chim Acta 449:96
16. Sartain HT, McGraw SN, Lawrence CL, Werner EJ, Biros SM (2015) Inorg Chim Acta 426:126
17. Matloka K, Sah AK, Peters MW, Srinivasan P, Gelis AV, Regalbuto M, Scott MJ (2007) Inorg Chem 46:10549
18. Sharova EV, Artyushin OI, Turanov AN, Karandashev VK, Meshkova SB, Topilova ZM, Odinets IL (2012) Centr Eur J Chem 10:146
19. Kudryavtsev IY, Baulina TV, Pasechnik MP, Aysin RR, Matveev SV, Petrovskii PV, Nifant'ev EE (2013) Russ Chem Bull 62:1086
20. Kudryavtsev IY, Baulina TV, Pasechnik MP, Matveev SV, Matveeva AG (2014) Phosphorus. Sulfur Silicon Relat Elem 189:946
21. Matveeva AG, Kudryavtsev IY, Pasechnik MP, Vologzhanina AV, Baulina TV, Vavina AV, Sukat GY, Matveev SV, Godovikov IA, Turanov AN, Karandashev VK, Brel VK (2018) Polyhedron 142:71
22. Turanov AN, Matveeva AG, Kudryavtsev IY, Pasechnik MP, Matveev SV, Godovikova MI, Baulina TV, Karandashev VK, Brel VK (2019) Polyhedron 161C:276
23. Dam HH, Reinhoudt DN, Verboom W (2007) Chem Soc Rev 36:367
24. Aromí G, Barrios LA, Roubeau O, Gamez P (2011) Coord Chem Rev 255:485
25. Huang D, Zhao P, Astru D (2014) Coord Chem Rev 272:145
26. Schulze B, Schubert US (2014) Chem Soc Rev 43:2522
27. Kacprzak K, Skiera I, Piasecka M, Paryzek Z (2016) Chem Rev 116:5689
28. Lukashev NV, Grabovyi GA, Erzunov DA, Kazantsev AV, Latyshev GV, Averin AD, Beletskaya IP (2017) Beilstein J Org Chem 13:564
29. Keivanloo A, Lashkari S, Sepehri S, Bakherad M, Abbaspour S (2020) Monatsh Chem 151:935
30. Schweinfurth D, Pattacini R, Strobel S, Sarkar B (2009) Dalton Trans 42:9291
31. Lo WKC, Huff GS, Cubanski JR, Kennedy ADW, McAdam CJ, McMorran DA, Gordon KC, Crowley JD (2015) Inorg Chem 54:1572
32. Hurtado J, Rojas RS, Pérez EG, Valderrama M (2013) J Chil Chem Soc 58:1534
33. Crowley JD, Gavey EL (2010) Dalton Trans 39:4035
34. Turanov AN, Karandashev VK, Artyushin OI, Sharova EV, Genkina GK, Yarkevich AN (2014) Solvent Extr Ion Exch 32:669
35. Nozoe A, Morisada S, Ohto K, Kawakita H (2014) Solvent Extr Ion Exch 33:56
36. Turanov AN, Karandashev VK, Sharova EV, Genkina GK, Artyushin OI (2015) RSC Adv 5:27640
37. Kudryavtsev IY, Bykhovskaya OV, Aladzheva IM, Baulina TV, Brel VK (2017) Russ J Gen Chem 87:2744
38. Livant PD, Mao J, Webb TR (1996) Acta Cryst C52:2924
39. Bykhovskaya OV, Matveeva AG, Pasechnik MP, Vologzhanina AV, Matveev SV, Kudryavtsev IY, Baulina TV, Brel VK (2019) Russ J Gen Chem 89:2400
40. Baulina TV, Kudryavtsev IY, Smolyakov AF, Pasechnik MP, Brel VK (2018) Heteroat Chem 29:e21454
41. Baulina TV, Pasechnik MP, Kudryavtsev IY, Bykhovskaya OV, Sukat GY, Smol'yakov AF, Anikina LV, Brel VK (2020) J Mol Struct 1217:128324
42. Pasechnik MP, Matveeva AG, Lyssenko KA, Aysin RR, Smol'yakov AF, Zubavichusc YV, Godovikov IA, Goryunov EI (2019) J Mol Struct 1175:874
43. Durrell AC, Gray HB, Hazari N, Incarvito CD, Liu J, Yan EC-Y (2010) Cryst Growth Des 10:1482
44. Nakamoto K (1997) IR and Raman Spectra of Inorganic and Coordination Compounds. Wiley, New York
45. Kozlov VA, Aleksanyan DV, Korobov MV, Avramenko NV, Aysin RR, Maloshitskaya OA, Korlyukov AS, Odinets IL (2011) Dalton Trans 40:8768
46. Armarego WLF (2017) Purification of Laboratory Chemicals. Elsevier, Amsterdam
47. Gel'man NE, Terent'eva EA, Shanina TM, Kiparenko LM, Rezl V (1987) Methods of Quantitative Organic Elemental Microanalysis. Khimiya, Moscow
48. Sheldrick GM (2015) Acta Cryst A71:3
49. Spek AL (2015) Acta Cryst C71:9
50. Sheldrick GM (2015) Acta Cryst C71:3
51. Dolomanov OV, Bourhis LJ, Gildea RJ, Howard JAK, Puschmann H (2009) J Appl Cryst 42:339